Journal of Superconductivity and Novel Magnetism (2021) 34:2293–2300
https://doi.org/10.1007/s10948-021-05880-4

ORIGINAL PAPER

Stress Analysis of Cylindrical Superconductors Based on Viscous Flux Flow and Flux Creep in the Demagnetization Process After ZFC

Wenhai Zhou[1,2] · Youhe Zhou[1] · Jiabao Hou[2]

Received: 18 January 2021 / Accepted: 30 March 2021 / Published online: 8 May 2021

Abstract
In this paper, the magnetoelastic problem of a long cylindrical superconductor placed in a time-dependent external magnetic field during the unloading phase after zero field cooling (ZFC) is investigated. The flux distribution equation considering the viscous flux flow effect and the flux creep effect is established, and the stress distribution equation of the long cylinder obtained by the strain method is modified on this basis. The results show that in the external magnetic field both viscous flux flow velocity and flux creep velocity will affect the stress distribution during low-frequency excitation, while the internal field flux distribution and stress distribution are mainly dominated by the viscous flux flow velocity during high-frequency excitation. In addition, the relationship between the viscous flux flow velocity and the external field excitation velocity and the relationship between the position r_0 and the magnitude $\sigma_{r,\ \max}(r)$ of the local stress peak and the action parameter (v_0, v_1, dB_a/dt, n) of the two effects are investigated.

Keywords Flux distribution · Viscous flux flow effect · Flux creep effect · The velocity of excitation · Local stress peak

1 Introduction

Bulk high-temperature superconductors have a high critical current density and a strong ability to trap magnetic fields at low temperatures, which makes it promising for a wide range of applications in many fields [1, 2]. However, bulk high-temperature superconductors are brittle materials, which are resistant to compression but not to tension. During the magnetization process, the performance of the bulks may weaken or fail due to the viscous flux flow effect of the external magnetic field and the flux creep effect of the internal field. Therefore, it is significant to study the effects of viscous flux flow and flux creep on the mechanical behavior of superconductors [3–5]. Anderson [6] conducted the first study of flux flow phenomena and used flux creep to explain the captured flux quantum escape within superconductors. Kim Y. B. [7] pointed out that the motion of flux quanta is mainly determined by the flux viscosity effect. P. H. et al. [8] first considered the viscous flux flow in the critical state Bean model. Liu Z. [9] combined the Bean model and the flux flow problem to obtain the analytical results of the flux distribution with respect to time, and the magnetization response of type II superconductors in the results is discussed. Inanir F. et al. [10] calculated the magnetostriction at different frequencies of the external magnetic field and concluded that the presence of high-frequency viscous flux flow can greatly enhance the magnitude of the magnetostrictive curves and change their shape. Xue F. et al. [11] considered the effects of flux creep and viscous flux flow on the flux motion and combined both effects for a comprehensive study of the magnetostriction phenomenon. Yang Yong et al. [12–15] first theoretically proposed an expression for the velocity of external magnetic field change and pointed out that the velocity of external magnetic field change has an effect on the velocity of viscous flux flow and the velocity of viscous flux flow has an effect on the internal stress distribution of bulk high-temperature superconductors. Although the concept of the velocity of change of the external magnetic field has been proposed, the problem is that the velocity of change of the external magnetic field during the magnetization process still does not visually reflect the flux creep effect, stress distribution

✉ Wenhai Zhou
18394499554@139.com

✉ Youhe Zhou
zhouyh@lzu.edu.cn

1 Key Laboratory of Mechanics on Environment and Disaster in Western China, The Ministry of Education of China, College of Civil Engineering and Mechanics, Lanzhou University, Lanzhou 730000, China

2 School of Petrochemical Technology, Lanzhou University of Technology, Lanzhou 730050, China

pattern, and the magnetostriction phenomenon inside the bulk high-temperature superconductors.

Based on the above work, this paper further investigates the mechanical behavior of type II long cylindrical superconductors during the drop of external magnetic field. The whole process considers the viscous flux flow effect as well as flux creep effect, and the flux distribution equation is modified, and finally the equation for the stress distribution of long cylinders is obtained. Based on which the effects of both effects on the flux distribution and stress distribution about time are discussed, as well as the relationship between the effect parameters and the flux distribution and local peak stress, this study has a theoretical direction for the application of superconducting materials.

2 Calculation of Stress in Bulk Cylindrical Superconductors

2.1 Flux Distribution Equation

A superconducting cylinder with a radius of R is placed in an external magnetic field B_a that changes with time, and the direction of the magnetic field is parallel to the z-axis. The model structure and the force acting on the cylindrical volume element are shown in Fig. 1. In order to obtain expressions for the internal stress distribution in cylindrical superconductors under viscous flux flow and flux creep effects, it is first necessary to determine the flux density distribution at each stage of the magnetization process.

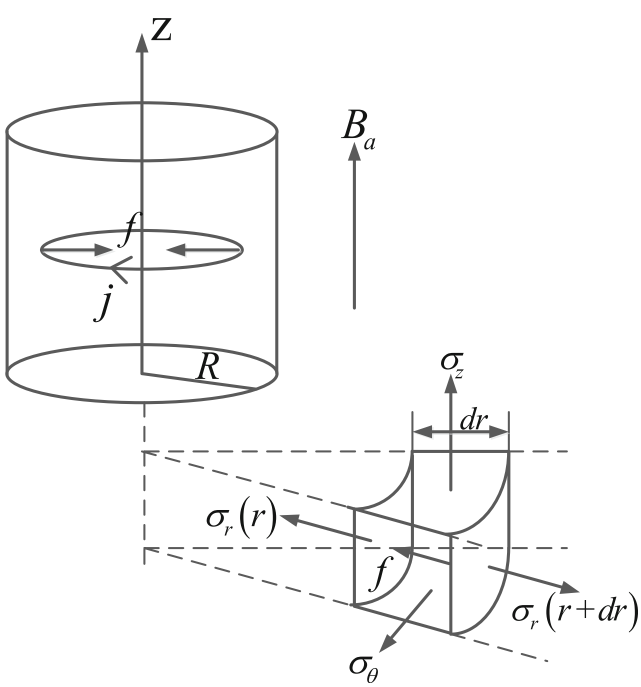

Fig. 1 Schematic drawing of an infinitely long cylindrical superconductor placed in a parallel field B_a pointing along the z-direction

At the viscous flux flow velocity, the flux distribution in the cylindrical superconductor obeys the following equation [16].

$$\frac{1}{\mu_0}\frac{\partial B}{\partial r} = \mp\left[J_c + \frac{\eta}{\phi}v(t)\right] \quad (1)$$

where J_c is a constant, η is the viscosity associated with flux motion, $v(t)$ is the velocity of the viscous flux flow, and ϕ_0 is the flux quantum. The $\mp$ corresponds to the rise (fall) of the magnetic field, respectively.

To ensure the conservation of magnetic flux, $v(t)$must also satisfy the flux continuity equation [8].

$$Bv = -\frac{\partial}{\partial t}\int_r^R B\left(r', t\right)dr' \quad (2)$$

A special solution can be obtained by Eq. (2).

$$B(r,t) = B(r - v_1 t) \quad (3)$$

Therefore, $v(t) = v_1$ satisfies the flux continuity (Eq. (2)). Substituting Eq. (3) into Eq. (1) for integration, the expression of the magnetic field distribution inside the superconductor can be obtained when the external magnetic field starts to decrease from the maximum value B_M. At this time, the boundary conditions are satisfied $t = 0$ and $B_a(t) = B_M$.

$$B(r,t) = B_a(t) - \mu_0\left(J_c + \frac{\eta}{\phi_0}\nu_1\right)(R - r) \quad (4)$$

Considering the effect of flux creep on the current density during the process of demagnetization, Shantsev et al [17] gave an exact solution of this problem.

$$J(r) = J_c(B_a/\mu_0 J_c v_0)^{1/n+1} \quad (5)$$

where $n = U_0/kT$ represents the chance of creep occurrence; v_0 is the velocity of the flux creep when the Lorentz force increases to equal the pinning force; for flux lines moving inside a superconductor, the part of the pinning center that plays a role in the pinning force density constitutes the effective pinning barrier, the average height of the barrier is U_0, and the flux line must overcome this barrier in order to move; T is the external field temperature; k is the Boltzmann constant; B_a is the speed of change of the external magnetic field.

Substituting J_c with $J(r)$ and putting it into Eq. (1), the magnetic flux distribution expression can be obtained by considering the viscous magnetic flux flow effect and the magnetic flux creep effect [18]:

$$\frac{1}{\mu_0}\frac{\partial B}{\partial r} = \mp\left[J_c\left(\dot{B}_a/\mu_0 J_c \nu_0\right)^{1/n+1} + \frac{\eta}{\phi_0}\nu_1\right] \quad (6)$$

Substituting Eq. (4) into Eq. (6) for integration, the equation of magnetic flux distribution within superconductor can be obtained during the demagnetization process of the external magnetic field starting from the maximum value $B_a = B_M$.

When $B^* < B_a \le B_M$, the internal magnetic field is divided into two parts, the non-activated region near the center of the superconductor and the active region near the edge of the superconductor.

$$B(r,t) = \begin{cases} B_M - \mu_0 J_c(R-r) & 0 \le r \le r_0 \\ B_a(t) + \mu_0\left[J_c\left(\dot{B}_a/\mu_0 J_c v_0\right)^{1/n+1} + \eta v_1/\phi_0\right](R-r) & r_0 \le r \le R \end{cases} \tag{7}$$

where B^* is the eigenvalue of the magnetic field when the current within superconductor is completely reversed during the drop of magnetic field and the physical force is completely changed to the tensile force. Solutions have to:

$$r_0 = R - \frac{B_a t}{\mu_0 J_c\left[(B_a/\mu_0 J_c v_0)^{1/(n+1)} + v_1/R + 1\right]} \tag{8}$$

$$B^* = B_M - \mu_0 J_c R\left[\left(\frac{B_a}{\mu_0 J_c v_0}\right)^{\frac{1}{n+1}} + \frac{v_1}{R} + 1\right] \tag{9}$$

When $B_a \le B^*$, the magnetic flux distribution in the superconductor is all transformed into an active state.

$$B(r,t) = B_a(t) + \mu_0\left(J_c(B_a/\mu_0 J_c v_0)^{1/(n+1)} + \eta v_1/\phi_0\right)(R-r) \quad 0 \le r \le R \tag{10}$$

2.2 Stress Distribution Equation

High-temperature superconductors are ceramic materials which are resistant to compression but not tensile, and the compressive strength is about five times higher than the tensile strength in the liquid nitrogen temperature region [5, 19]. During the magnetization process, the compressive stress is applied to the inside of high-temperature superconductor bulks during the rising phase of the magnetic field, and the internal compressive stress gradually changes to tensile stress during the unloading phase of the magnetic field. In order to study the effect of external magnetic field variation on the safety of superconductor structure, only the process of unloading magnetization of external magnetic field at different speeds is considered in this paper for stress analysis.

Tom H. Johansen [20] gave the internal stress expression of a long cylindrical superconductor with the variation of external magnetic field as:

$$\begin{cases} \sigma_r(r) = \frac{1}{2\mu_0}\left[B^2 - B_a^2 + \frac{1-2\upsilon}{1-\upsilon}\left(\int_0^1 \rho' B^2(r) d\rho' - \frac{1}{\rho^2}\int_0^\rho \rho' B^2(r) d\rho'\right)\right] \\ \sigma_\theta(r) = \frac{1}{2\mu_0}\left[\frac{\upsilon}{1-\upsilon} B^2 - B_a^2 + \frac{1-2\upsilon}{1-\upsilon}\left(\int_0^1 \rho' B^2(r) d\rho' - \frac{1}{\rho^2}\int_0^\rho \rho' B^2(r) d\rho'\right)\right] \end{cases} \tag{11}$$

In order to simplify the calculation, some parameters are non-dimensionalized, $b = B/B_p$, $b_a = B_a/B_p$, $b_m = B_M/B_p$, $\rho_0 = r_0/R$, $\sigma_0 = B_p^2/2\mu_0$, $\gamma = \eta v_1/(J_c\phi_0) = v_1/R$, and $K = B_a/\mu_0 J_c v_0$. Incorporating Eq. (7) and Eq. (10) into Eq. (11) to calculate [14]:

When $B^* < B_a \le B_M$, $0 < \rho \le \rho_0$:

$$\begin{aligned} \frac{\sigma_r}{\sigma_0} = b^2 - b_a^2 + \frac{1-2\upsilon}{1-\upsilon}&\left\{\frac{1}{4}\rho_0^4 + \frac{2}{3}(b_m-1)\rho_0^3 + \frac{1}{2}(b_m-1)^2\rho_0^2\right\} \\ &+ \frac{1}{4}\left(K^{\frac{1}{(n+1)}} + \gamma\right)^2(1-\rho_0^4) - \frac{2}{3}\left(K^{\frac{1}{(n+1)}} + \gamma\right)\left[b_a + \left(K^{\frac{1}{(n+1)}} + \gamma\right)\right](1-\rho_0^3) \\ &+ \frac{1}{2}\left[b_a + \left(K^{\frac{1}{(n+1)}} + \gamma\right)\right]^2(1-\rho_0^2) - \left[\frac{1}{4}\rho^2 + \frac{2}{3}(b_m-1)\rho + \frac{1}{2}(b_m-1)^2\right]\Big\} \end{aligned} \tag{12}$$

$$\begin{aligned} \frac{\sigma_\theta}{\sigma_0} = \frac{\upsilon}{1-\upsilon} b^2 - b_a^2 + \frac{1-2\upsilon}{1-\upsilon}&\left\{\frac{1}{4}\rho_0^4 + \frac{2}{3}(b_m-1)\rho_0^3 + \frac{1}{2}(b_m-1)^2\rho_0^2\right. \\ &+ \frac{1}{4}\left(K^{\frac{1}{(n+1)}} + \gamma\right)^2(1-\rho_0^4) - \frac{2}{3}\left(K^{\frac{1}{(n+1)}} + \gamma\right)\left[b_a + \left(K^{\frac{1}{(n+1)}} + \gamma\right)\right](1-\rho_0^3) \\ &\left.+ \frac{1}{2}\left[b_a + \left(K^{\frac{1}{(n+1)}} + \gamma\right)\right]^2(1-\rho_0^2) + \left[\frac{1}{4}\rho^2 + \frac{2}{3}(b_m-1)\rho + \frac{1}{2}(b_m-1)^2\right]\right\} \end{aligned} \tag{13}$$

When $B^* < B_a \le B_M$, $0 < \rho \le 1$:

$$\begin{aligned} \frac{\sigma_r}{\sigma_0} = b^2 - b_a^2 + \frac{1-2\upsilon}{1-\upsilon}&\left\{\frac{1}{4}\rho_0^4 + \frac{2}{3}(b_m-1)\rho_0^3 + \frac{1}{4}\left(K^{\frac{1}{(n+1)}} + \gamma\right)^2(1-\rho_0^4)\right. \\ &+ \frac{2}{3}\left(K^{\frac{1}{(n+1)}} + \gamma\right)\left[b_a + \left(K^{\frac{1}{(n+1)}} + \gamma\right)\right](1-\rho_0^3) + \frac{1}{2}\left[b_a + \left(K^{\frac{1}{(n+1)}} + \gamma\right)\right]^2(1-\rho_0^2) \\ &+ \frac{1}{\rho^2}\left[\frac{1}{4}\rho_0^4 + \frac{2}{3}(b_m-1)\rho_0^3 + \frac{1}{2}(b_m-1)^2\rho_0^2\right] - \frac{1}{\rho^2}\left[\frac{1}{4}\left(K^{\frac{1}{(n+1)}} + \gamma\right)^2(b^4-\rho_0^4)\right] \\ &\left.- \frac{2}{3}\left(K^{\frac{1}{(n+1)}} + \gamma\right)\left[b_a + \left(K^{\frac{1}{(n+1)}} + \gamma\right)\right](b^3-\rho_0^3) + \frac{1}{2}\left[b_a + \left(K^{\frac{1}{(n+1)}} + \gamma\right)\right]^2(b^2-\rho_0^2)\right\} \end{aligned} \tag{14}$$

$$\begin{aligned} \frac{\sigma_\theta}{\sigma_0} = \frac{\upsilon}{1-\upsilon} b^2 - p_a^2 + \frac{1-2\upsilon}{1-\upsilon}&\left\{\frac{1}{4}\rho_0^4 + \frac{2}{3}(b_m-1)\rho_0^3 + \frac{1}{2}(b_m-1)\rho_0^2 + \frac{1}{4}\left(K^{\frac{1}{(n+1)}} + \gamma\right)^2(1-\rho_0^4)\right. \\ &+ \frac{2}{3}\left(K^{\frac{1}{(n+1)}} + \gamma\right)\left[b_a + \left(K^{\frac{1}{(n+1)}} + \gamma\right)\right](1-\rho_0^3) + \frac{1}{2}\left[b_a + \left(K^{\frac{1}{(n+1)}} + \gamma\right)\right]^2(1-\rho_0^2) \\ &+ \frac{1}{\rho^2}\left[\frac{1}{4}\rho_0^4 + \frac{2}{3}(b_m-1)\rho_0^3 + \frac{1}{2}(b_m-1)^2\rho_0^2\right] - \frac{1}{\rho^2}\left[\frac{1}{4}\left(K^{\frac{1}{(n+1)}} + \gamma\right)^2(b^4-p_0^4)\right] \\ &\left.- \frac{2}{3}\left(K^{\frac{1}{(n+1)}} + \gamma\right)\left[b_a + \left(K^{\frac{1}{(n+1)}} + \gamma\right)\right](b^3-p_0^3) + \frac{1}{2}\left[b_a + \left(K^{\frac{1}{(n+1)}} + \gamma\right)\right]^2(b^2-p_0^2)\right\} \end{aligned} \tag{15}$$

When $B_a \le B^*$, $0 \le \rho \le 1$:

$$\frac{\sigma_r}{\sigma_0} = b^2 - b_a^2 + \frac{1-2\upsilon}{1-\upsilon}\left\{\frac{1}{4}\left(K^{\frac{1}{(n+1)}}+\gamma\right)^2 - \frac{2}{3}\left(K^{\frac{1}{(n+1)}}+\gamma\right)\left[b_a+\left(K^{\frac{1}{(n+1)}}+\gamma\right)\right]+\frac{1}{2}\left[b_a+\left(K^{\frac{1}{(n+1)}}+\gamma\right)\right]^2 \right. \\ \left. -\frac{1}{4}\left(K^{\frac{1}{(n+1)}}+\gamma\right)^2\rho^2 - \frac{2}{3}\left(K^{\frac{1}{(n+1)}}+\gamma\right)\left[b_a+\left(K^{\frac{1}{(n+1)}}+\gamma\right)\right]\rho + \frac{1}{2}\left[b_a+\left(K^{\frac{1}{(n+1)}}+\gamma\right)^2\right]\right. \tag{16}$$

$$\frac{\sigma_\theta}{\sigma_0} = \frac{\upsilon}{1-\upsilon}b^2 - b_a^2 + \frac{1-2\upsilon}{1-\upsilon}\left\{\frac{1}{4}\left(K^{\frac{1}{(n+1)}}+\gamma\right)^2 - \frac{2}{3}\left(K^{\frac{1}{(n+1)}}+\gamma\right)\left[b_a+\left(K^{\frac{1}{(n+1)}}+\gamma\right)\right]+\frac{1}{2}\left[b_a+\left(K^{\frac{1}{(n+1)}}+\gamma\right)\right]^2 \right. \\ \left. +\frac{1}{4}\left(K^{\frac{1}{(n+1)}}+\gamma\right)^2\rho^2 - \frac{2}{3}\left(K^{\frac{1}{(n+1)}}+\gamma\right)\left[b_a+\left(K^{\frac{1}{(n+1)}}+\gamma\right)\right]\rho + \frac{1}{2}\left[b_a+\left(K^{\frac{1}{(n+1)}}+\gamma\right)^2\right]\right. \tag{17}$$

3 Flux Flow Effect

When $K = 0.5$, $n = 3$, $v_1/R = 1$, and $\upsilon = 0.3$, according to Eq. (9), $B^* = 1.156B_p$ is obtained. When the external magnetic field B_a decreases in the range of $B^* < B_a \le B_M$, if the external magnetic field B_a is taken as a fixed value, the radial stress σ, (r) in the superconductor first increases until the critical current changes and reaches the maximum value and then decreases. During the falling of the external magnetic field, $\sigma_r(r)$ gradually becomes tensile stress on the outside of the cylinder. As the edge is re-magnetized, the position r_0 where the local peak $\sigma_{r,\ \max}(r)$ appears moves toward the center of the superconductor. During the movement, $\sigma_{r,\max}(r)$ shows an increasing trend, and the magnetic flux density at this point is also the largest. At this stage, there is a coexistence phenomenon of tensile stress and compressive stress, and $B_a = 3.13B_p$ is the demarcation point of the direction of $\sigma_r(r)$; at this time, $\sigma_r(r)$ is completely transformed into tensile force; when $B_a = B^*$, $r_0 = 0$, at which, $\sigma_{r,\ \max}(r)$ reaches the maximum value; that is, the maximum tensile stress peak appears at the center of the cylindrical superconductor; when B_a drops to the range of $0 \le B_a < B^*$, $\sigma_r(r)$ gradually decreases with the decrease of the external magnetic field B_a. When the external magnetic field B_a takes a fixed value at this stage, $\sigma_r(r)$ tends to decrease throughout the superconductor and still shows a tensile phenomenon. By observing Fig. 2, $\sigma_\theta(r)$ shows the same distribution law as $\sigma_r(r)$. The difference is that at $r_0 = 1$, $\sigma_r(r)$ is all reduced to zero, while $\sigma_\theta(r)$ is not completely reduced to zero, and $\sigma_\theta(r)$ remains at the edge of the superconducting cylinder.

3.1 Stress Distribution at Different Viscous Flux Flow Velocities

When $B_a = 3.5B_p$, $\sigma_r(r)$ in the superconductor is in a state of coexistence of tension and compression, but when $B_a = 0$, $\sigma_r(r)$ in the superconductor is in a fully tensile state. Similarly, take $K = 0.5$ and $n = 3$ as constant values, and discuss the stress distribution of the external magnetic field under the different viscous lux flow velocity.

When the external magnetic field drops from $B_a = B_M$ to $B_a = 3.5B_p$ and $B_a = 0$, by varying v_1, it is found that as v_1 increases, $\sigma_r(r)$ increases gradually under the two different external magnetic field conditions, and $\sigma_{r,\ \max}(r)$ also shows an increasing trend and moves to the outside of the superconductor. It is worth noting that when $B_a = 3.5B_p$, regardless of the value of v_1, $\sigma_r(r)$ in the superconductor always increases first and then decreases with the increase of r. However, when $B_a = 0$, if the value of v_1 is larger, the change trend of $\sigma_r(r)$ is consistent with that of $B_a = 3.5B_p$; while the value of v_1 is smaller, $\sigma_r(r)$ only shows a gradual decrease. $\sigma_\theta(r)$ presents the same distribution law as $\sigma_r(r)$, except that no matter what value v_1 takes, $\sigma_r(r)$ drops to zero at the edge of the superconductor, while $\sigma_\theta(r)$ appears residual.

3.2 Stress Distribution Under Different External Field Excitation Velocities

Assuming that the flux creep effect in the superconductor is not considered during the excitation of external magnetic field, at this time, $|dB_a/dt| = \mu_0(J_c + \eta v_1 \phi_0)v_1$, $B_p = \mu_0 J_c R$, so $|db_a/dt| = (dB_a/B_p)/dt = (v_1/R)(1 + v_1/R)$, where v_1 is mainly determined by the external magnetic field excitation velocity $b_a = db_a/dt$, and the two are in a square relationship. However, v_1 is difficult to control in actual operation under an alternating field, so it is more valuable to use the change of $b_a = db_a/dt$ instead of the change of v_1 to analyze the superconductor stress distribution. Since the changing laws of $\sigma_r(r)$ and $\sigma_\theta(r)$ are basically the same, only the relationship between $\sigma_r(r)$ and db_a/dt is discussed.

The comparison of Figs. 3 and 4 reveals that if the functional relationship between v_1 and db_a/dt is considered, the variation law of $\sigma_r(r)$ under different external magnetic field conditions should be consistent, which will not be described more here.

3.3 The Distribution of Stress Local Peak

When the tensile stress in the superconductor reaches a local peak, it poses a serious threat to the safety of the

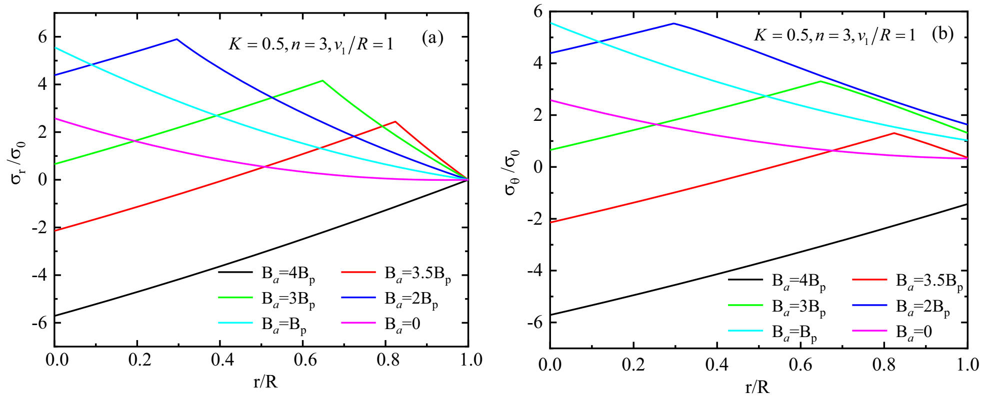

Fig. 2 Stress profiles as the applied field is decreased from $B_a = 4B_p$ to $B_a = 3.5B_p$, $B_a = 3B_p$, $B_a = 2B_p$, $B_a = B_p$, and $B_a = 0$ for $K = 0.5$, $n = 3$, and $v_1/R = 1$. (**a**) Radial stress distribution curve. (**b**) Hoop stress distribution curve

superconductor structure, so we are more concerned about the distribution of the maximum local tensile stress $\sigma_{r,\ max}(r)$ during the excitation process. In the process of external magnetic field excitation, for different external magnetic field conditions, when $r = r_0$, $\sigma_r(r)$ has a local peak value $\sigma_{r,\ max}(r) = \sigma(r_0)$. Substituting Eq. (8) into Eq. (7) yields $B(r_0, t) = B_M - (B_M - B_a)/[(B_a/\mu_0 J_c v_0)^{1/(n+1)} + v_1/R + 1]$, and then putting $B(r_0, t)$ into Eq. (11) yields $\sigma_{r,\max}(r)/\sigma_0 = [(2-3\upsilon)/(1-\upsilon)]b^2(r_0, t) - b_a^2$. The distribution of $\sigma_{r,\ max}(r)$ in the superconductor is observed by changing db_a/dt.

The analysis of Fig. 5 shows that, as db_a/dt increases, $\sigma_{r,\ max}(r)$ tends to increase and then decrease throughout the unloading phase of the magnetic field. And when the value of db_a/dt is small, the superconductor excitation phenomenon is equivalent to the quasi-static state, and the increase of $\sigma_{r,\ max}(r)$ is relatively slow, but when the value of db_a/dt is large, $\sigma_{r,\ max}(r)$ increases significantly. Therefore, to ensure the safety of the superconductor structure, it is necessary to control db_a/dt should not be too large.

4 Flux Creep Effect

4.1 The Influence of Flux Flow and Flux Creep on Local Stress Peak

The dimensionless quantity $v' = \mu_0 J_c v_0/B_a$ is chosen to characterize the flux creep effect. When the external magnetic field

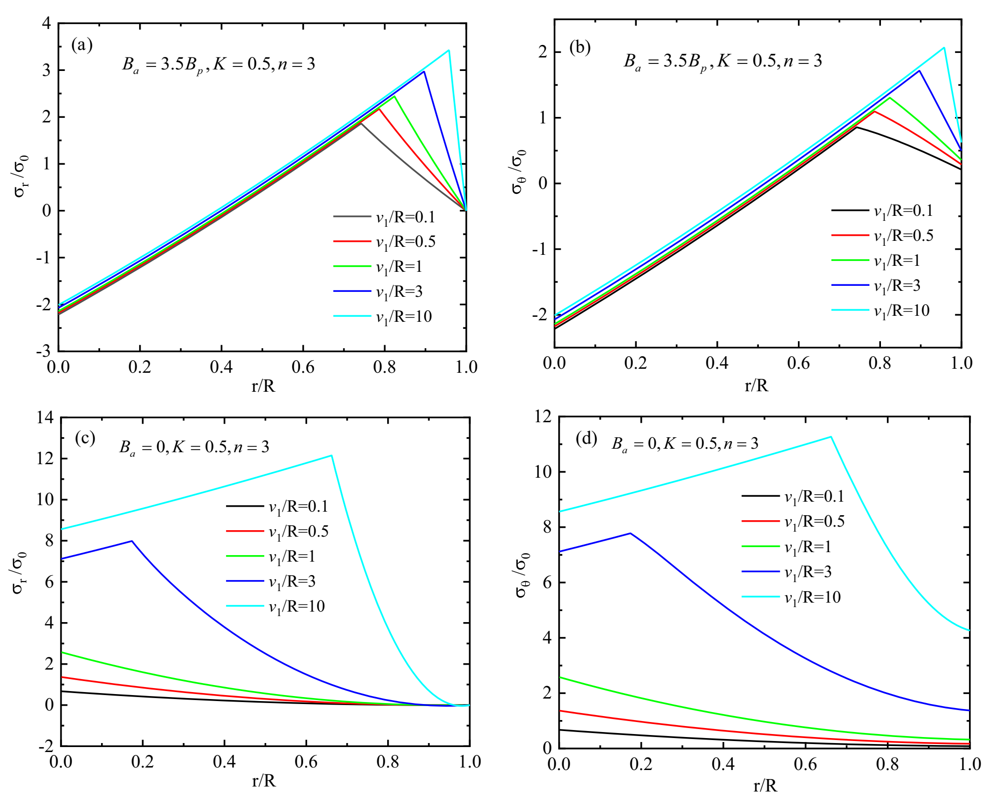

Fig. 3 Stress profiles as the applied field is decreased from $B_a = 4B_p$ to $B_a = 3.5B_p$ and $B_a = 0$ for $v_1/R = 0.1$, $v_1/R = 0.5$, $v_1/R = 1$, $v_1/R = 3$, and $v_1/R = 10$. (**a**, **b**) Radial and hoop stress distributions when $v_1/R = 3.5B_p$. (**c**, **d**) Radial and hoop stress distributions when $B_a = 0$

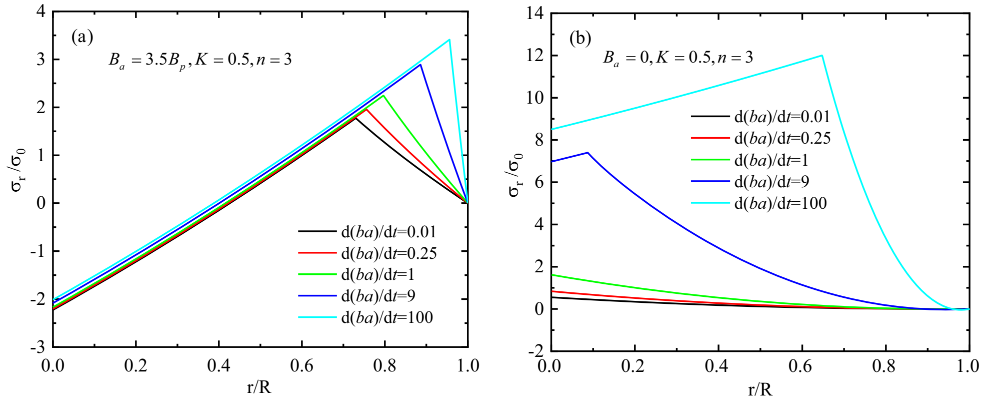

Fig. 4 Relationship between maximum radial tensile stress and values of db_a/dt as the applied field is decreased from $B_a = 4B_p$ to $B_a = 3.5B_p$ and $B_a = 0$. (**a**) $B_a = 3.5B_p$. (**b**) $B_a = 0$

decreases to $B_a = 3.5B_p$ and $B_a = 0$, the variation of v_1/R with $\sigma_{r,\ \max}(r)$ are generally the same for different value of v'. $\sigma_{r,\ \max}(r)$ gradually increases with the increase of v_1/R, and the gradient of the increasing speed gradually slows down, and finally $\sigma_{r,\ \max}(r)$ tends to stabilize when v_1/R takes a value within a larger value range and reaches a common extreme value. It is worth noting that when the value of v_1/R is small, the change of $v^{'}$ has a great influence on $\sigma_{r,\ \max}(r)$; when the value of v_1/R is large, the influence of the change of $v^{'}$ on $\sigma_{r,\ \max}(r)$ can be ignored. Obviously, during the low-frequency excitation of the external magnetic field, the variations of v_1/R and $v^{'}$ will have a greater impact on $\sigma_{r,\ \max}(r)$; while during the high-frequency excitation of the external magnetic field, only v_1/R will dominate the motion of the flow field, which in turn determines the flux distribution within the superconductor and ultimately the stress distribution within the superconductor. The relationship between maximum radial tensile stresses the applied field and the viscous flux flow velocity is shown in Fig. 6.

Figure 7 shows that the external magnetic field respectively decreases to $B_a = 3.5B_p$ and $B_a = 0$, and the variation of $\sigma_{r,\ \max}(r)$ with $v^{'}$ is approximately the same when the probability n of creep occurrence is taken to different values. When $v' < 1$, $\sigma_{r,\ \max}(r)$ gradually decreases as the value of n increases, and the decreasing velocity gradient gradually slows down, until n takes a value in a larger range, $\sigma_{r,\ \max}(r)$ will tend to be stable. When $v' < 1$, $\sigma_{r,\ \max}(r)$ gradually increases as the value of n increases, the increasing velocity gradient gradually slows down and finally stabilizes. When $v' > 1$, no matter what the value of n is, $\sigma_{r,\ \max}(r)$ is equal, which indicates that the current model considering the creep effect at $v' = 1$ is equivalent to the critical state model (Bean). Therefore, in the actual excitation process, especially when the alternating magnetic field is applied, the critical state model is used to calculate the stress level of the superconductor, which will cause large errors in the results. It can be seen from Eq. (5) that when $v' < 1$, $J(r) > J_c$, and when $v' > 1$, $J(r) < J_c$. Therefore, for $v' > 1$, $\sigma_{r,\ \max}(r)$ can be reduced by decreasing the value of n. Since $n = U_0/kT$, it means that when $v' < 1$, the low barrier height and high-temperature conditions can improve the safety of the superconductor structures, while the situation is the opposite when $v' < 1$. Therefore, it is necessary to consider the influence of flux creep in the stress analysis, especially for high-temperature type II superconductors.

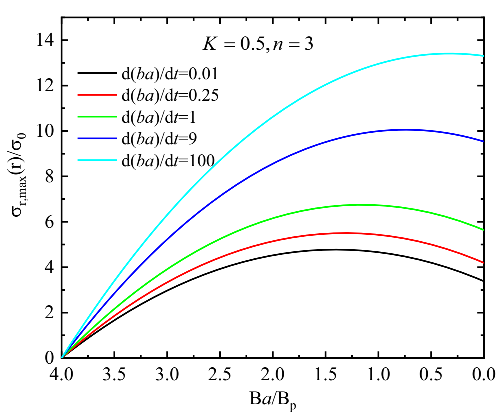

Fig. 5 The maximum radial tensile versus the applied field with the different values of db_a/dt

4.2 The Relationship Between the Position of the Local Stress Peak and the Effect Parameters Under Different External Fields

In stress analysis of superconductors, we not only pay attention to the distribution of stress in superconductor but also more concern about where the earliest threats to the safety of the superconductor structure appear. Therefore, it is necessary to discuss the variation of the position r_0 where the superconductor stress has a local peak $\sigma_{r,\ \max}(r)$ with external field conditions.

Figure 8a shows the variation of r_0 with v_1/R when v' takes different values. No matter what value v' takes, the position r_0 moves toward the edge of the superconductor as v_1/R increases and finally fixes at a specific

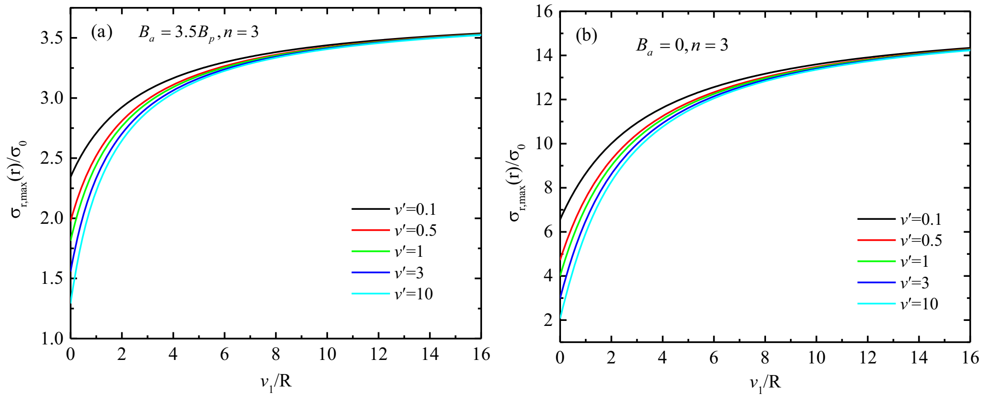

Fig. 6 Relationship between maximum radial tensile stresses the applied field and values of v_1/R for different values of v' and $n = 3$. (**a**) $B_a = 3.5B_p$. (**b**) $B_a = 0$

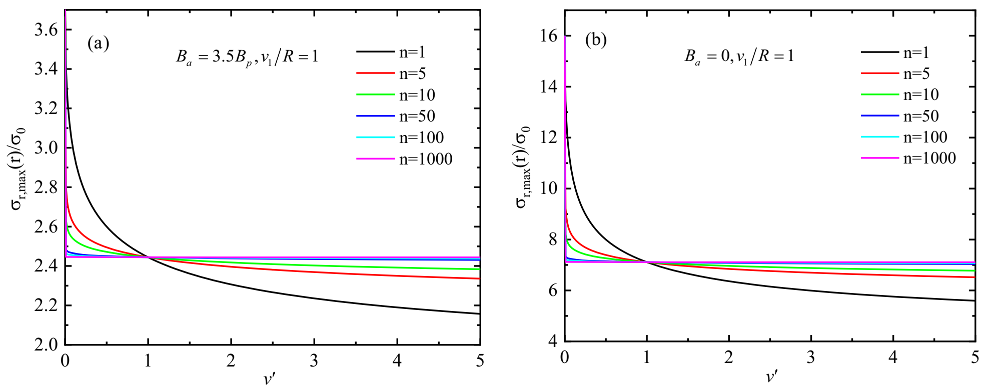

Fig. 7 Relationship between maximum radial tensile stresses the applied field and values of v' for different values of n and $v_1/R = 1$. (**a**) $B_a = 3.5B_p$. (**b**) $B_a = 0$

position. When v_1/R takes a fixed value in a relatively small value range, if the value of v' is increased, r_0 tends to move toward the center of the superconductor. Figure 8b shows the relationship between the position r_0 and v' when the probability of creep occurrence n is different. When $v' \leq 1$, the position of r_0 moves toward the center of the superconductor as the value of n increases; when $v' > 1$, the position of r_0 moves toward the edge of superconductor as the value of n increases; when n is infinitely large, no matter what value v' takes, the position of r_0 tends to a certain value and no longer varies with v'. This means that the position where $\sigma_{r,max}(r)$ appears in the superconductor is a certain value under the condition of larger barrier height U_0 and low temperature.

5 Conclusion

In this paper, based on the viscous flux flow effect and the flux creep effect, the magnetic flux distribution equation with respect to time is established, and the stress distribution function in a cylindrical superconductor with gradually decreasing external field after zero field cooling (ZFC) is solved. The distribution law of stress in the two states of whether the current is completely reversed during the field reduction process is

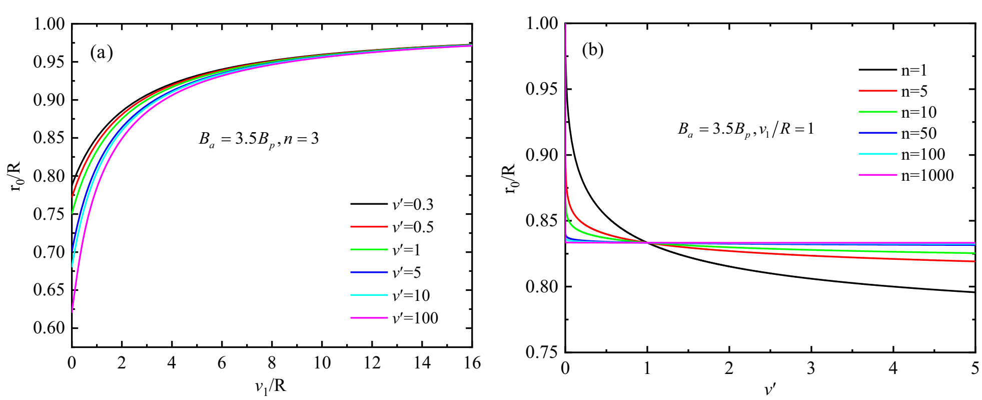

Fig. 8 Variation in the position r_0/R for different values of v_1/R and v'. (**a**) Relationship between r_0/R and v_1/R for different values of v' and $B_a = 3.5B_p$, $n = 3$. (**b**) Relationship between r_0/R and v' for different values of n and $B_a = 3.5B_p$, v_1/R

analyzed, and the interrelationship between the position r_0 as well as the magnitude $\sigma_{r,\ \max}(r)$ of the local stress peak and the action parameters (v_0, v_1, dB_a/dt, n) of the two effects are analyzed.

(1) During the low-frequency excitation of the external magnetic field, the changes of v'/R and v' will have a greater impact on $\sigma_{r,\ \max}(r)$, while during the high-frequency excitation of the external magnetic field, only v_1/R will dominate the motion of the flow field, which in turn determines the flux distribution within the superconductor and ultimately the state of the stress distribution within the superconductor.

(2) The probability of creep occurrence $n = 3$ is fixed, no matter what value v' takes, $\sigma_{r,\ \max}(r)$ increases with the increase of v_1/R, and finally stabilizes to a common extreme value. The position r_0 moves toward the edge of the superconductor with the increase of v_1/R and finally is also fixed at a specific position. When v_1/R takes a smaller value, the change of v' will have a great impact on $\sigma_{r,\ \max}(r)$. If the value of v_1/R is fixed at this time, as v' increases, r_0 will tend to move to the center of the superconductor; when v_1/R takes a larger value, the impact of v' change on $\sigma_{r,\ \max}(r)$ can be negligible.

(3) Take $v_1/R = 1$ as a fixed value. When $v' < 1$, as the value of n increases, $\sigma_{r,\ \max}(r)$ gradually decreases, the position of r_0 moves toward the center of the superconductor, and finally both tend to stabilize; when $v' > 1$, the situation is the opposite; when $v' = 1$, no matter what the value of n takes, $\sigma_{r,\ \max}(r)$ is the equal; and when the value of n is infinite, no matter what the value of v' takes, the position of r_0 tends to a certain value and no longer changes with the change of v'.

References

1. Deng, Z., Tsuzuki, K., Miki, M., et al.: Relaxation properties of the trapped flux of bulk high-temperature superconductors at different magnetization levels. J. Supercond. Nov. Magn. **25**, 331–338 (2012)
2. Yong, H.D., Zhou, Y.H., Zeng, J.: Crack problem in a long cylindrical superconductor. J. Appl. Phys. **104**, 448 (2008)
3. Srivastava, S.K., Aghajamali, A.: Analysis of reflectance properties in 1d photonic crystal containing metamaterial and high-temperature superconductor. J. Supercond. Nov. Magn. **30**(2), 343–351 (2017)
4. Wang, T.G., Li, Z.X., Cao, J.J., et al.: Mechanical damage of YBa2Cu3O7 coated conducting film caused by its CeO2 interface with defects. Int. J. Appl. Mech. **11**, 1950038 (2019)
5. Yang, Y., Chai, X.G.: Viscous flux flow velocity and stress distribution in the Kim model of a long rectangular slab superconductor. Supercond. Sci. Technol. **31**, 055005 (2018)
6. Anderson, P.W.: Theory of flux creep in hard superconductors. Phys. Rev. Lett. **9**, 309–311 (1962)
7. Kim, Y.B., Hempstead, C.F., Strnad, A.R.: Flux-flow resistance in type-II superconductors. Solid State Commun. **65**, 1171–1173 (1965)
8. Melville, P.H.: Effect of viscous forces in type II superconductors under A. C. conditions. Phys. Lett. A. **39**, 373–374 (1972)
9. Liu, Z., Bowden, G.J.: Viscous flux flow in the Bean model of type II superconductors. Supercond. Sci. Technol. **4**, 122 (1991)
10. Inanir, F., Celebi, S., Altunbas, M., et al.: Critical state magnetostriction of type-II superconductors under viscous flux flow. Phys. C: Supercond. **459**, 11–17 (2007)
11. Xue, F., Yong, H.D., Zhou, Y.H.: Effect of flux creep and viscous flux flow on flux-pinning-induced stress and magnetostriction in a long rectangular slab superconductor. J. Appl. Phys. **108**, 448 (2010)
12. Yang, Y., Xiao, L.Y., Li, X.H.: Impact of viscous flux flow on the stress in long rectangular slab superconductors. J. Appl. Phys. **107**, 517 (2010)
13. Yang, Y., Xiao, L.Y., Li, X.H., et al.: Stress in bulk type-II superconductor under viscous flux motion for a complete field cycle after zero-field cooling. IEEE Trans. Appl. Supercond. **20**, 1507–1510 (2010)
14. Yang, Y., Zhang, G.M., Wang, L., et al.: Impact of viscous flux flow on the stresses in long cylindrical superconductors. Supercond. Sci. Technol. **24**, 095003 (2011)
15. Yang, Y., Zheng, X.: Radial and hoop compressive stresses in a long cylindrical superconductor with viscous flux flow. J. Supercond. Nov. Magn. **28**, 2255–2258 (2015)
16. Zhao, Y.F., Xiong, K.: Magnetization and stress in superconducting 467 film under electromagnetic force with viscous flux flow. Mod. 468 Phys. Lett. B. 34,2050283 (2020)
17. Shantsev, D.V., Galperin, Y.M., Johansen, T.H.: Scaling and exact solutions for the flux creep problem in a slab superconductor. Phys. Rev. B. **65**, 184512 (2002)
18. Zhao, Y., Ji, P.: Crack problem in a slab superconductor under flux creep and viscous flux flow after zero field cooling. Phys. C: Supercond. Appl. **579**, 1353772 (2020)
19. Sakai, N., Mase, A., Ikuta, H., et al.: Mechanical properties of Sm-476 Ba-Cu-O/Ag bulk superconductors. Supercond. Sci. Technol. 13,770–773 (2000)
20. Johansen, T.H.: Flux-pinning-induced stress and strain in superconductors: Case of a long circular cylinder. Phys. Rev. B. **60**, 9690 (1999)